Quantitative Cell-Based Reporter Gene Assays Using Droplet-Based Microfluidics

Jean-Christophe Baret,[1,3,4,*] Yannick Beck,[1,2,3] Isabelle Billas-Massobrio,[2] Dino Moras,[2] and Andrew D. Griffiths[1,*]

[1]Institut de Science et d'Ingénierie Supramoléculaires (ISIS), Université de Strasbourg, CNRS UMR 7006, 8 Allée Gaspard Monge, BP 70028, F-67083 Strasbourg Cedex, France
[2]Institut de Génétique et de Biologie Moléculaire et Cellulaire (IGBMC), Département de Biologie et de Génomique Structurales, F-67400 Illkirch, France
[3]These authors contributed equally to this work
[4]Present address: Max Planck Institute for Dynamics and Self-Organisation, Bunsenstrasse 10, D-37073 Göttingen, Germany
*Correspondence: jc.baret@unistra.fr (J.-C.B.), griffiths@unistra.fr (A.D.G.)

SUMMARY

We used a droplet-based microfluidic system to perform a quantitative cell-based reporter gene assay for a nuclear receptor ligand. Single *Bombyx mori* cells are compartmentalized in nanoliter droplets which function as microreactors with a >1000-fold smaller volume than a microtiter-plate well, together with eight or ten discrete concentrations of 20-hydroxyecdysone, generated by on-chip dilution over 3 decades and encoded by a fluorescent label. The simultaneous measurement of the expression of green fluorescent protein by the reporter gene and of the fluorescent label allows construction of the dose-response profile of the hormone at the single-cell level. Screening ∼7500 cells per concentration provides statistically relevant data that allow precise measurement of the EC_{50} (70 nM ± 12%, α = 0.05), in agreement with standard methods as well as with literature data.

INTRODUCTION

Cell-based assays are an essential tool for chemical biology and chemical genetics approaches to identify new drug targets and molecules of potential medical value, as exemplified in the HIV field (Pauwels, 2006). Indeed, cell-based assays now represent approximately half of all screens performed (An and Tolliday, 2009). However, despite the fact that it has been known for many years that the biological effects of chemical compounds can display complex concentration-dependent relationships (Hill, 1910) varying in potency, efficacy, and steepness of response, usually just a single measurement at a single concentration (typically 10 μM) is obtained for each compound in a primary screen. This results in high numbers of false positives and false negatives (Malo et al., 2006) as well as the inability to identify subtle complex pharmacology, such as partial agonism or antagonism. These problems can be overcome by generating dose-response profiles for each compound in a library, for example by robotic plating of compounds in 1536-well plates (Inglese

et al., 2006). However, the number of cells required to generate dose-response profiles in this format can be prohibitive: it may be too expensive to produce the cells required and, some cells, for example human primary cells, may simply not be available in sufficient quantity. Reducing assay volumes below the 1-2 μl capacity of 1536-well plates is problematic due to evaporation and capillary forces (Dove, 1999). It is therefore extremely important to develop fast, quantitative, and reliable techniques for cell-based assays which allow the measurement of dose-response profiles using only small amounts of reagents and small numbers of cells. In this respect, microfluidic systems, in which mammalian cells can be both cultivated and assayed, present a promising alternative to conventional plate-based systems (Wu et al., 2010).

Here we describe a droplet-based microfluidic system for the precise measurement of dose-response profiles at the single-cell level using a reporter gene assay. In droplet-based microfluidic systems (Huebner et al., 2008), aqueous microdroplets dispersed in an immiscible carrier oil act as the functional equivalent of microtiter-plate wells (Tawfik and Griffiths, 1998; Griffiths and Tawfik, 2006). These systems appear attractive for quantitative cell-based screening for several reasons (Kelly et al., 2007; Hong et al., 2009). First, compartmentalization in droplets prevents diffusion and Taylor-Aris dispersion of reagents (Taylor, 1953; Squires and Quake, 2005). Second, highly monodispersed droplets can be created (Anna et al., 2003), split (Song et al., 2003; Link et al., 2004; Ménétrier-Deremble and Tabeling, 2006), fused (Chabert et al., 2005; Ahn et al., 2006a; Priest et al., 2006), incubated (Song and Ismagilov, 2003; Frenz et al., 2009), and sorted (Ahn et al., 2006b) in a controlled manner, all at rates of at least 1000 droplets per second (Griffiths and Tawfik, 2006), and multiple sequential operations on droplets can be combined to perform, for example, multistep reactions (Mazutis et al., 2009) or fluorescence-activated cell sorting (Baret et al., 2009; Agresti et al., 2010; Granieri et al., 2010). Third, human cells can be encapsulated in droplets (Clausell-Tormos et al., 2008; Köster et al., 2008; Chabert and Viovy, 2008; Brouzes et al., 2009; Hufnagel et al., 2009; Joensson et al., 2009) and remain highly viable for several days, allowing assays for cellular enzymatic activity and viability to be performed (Clausell-Tormos et al., 2008; Brouzes et al., 2009).

We measure the dose-reponse curve for a nuclear receptor agonist, the insect hormone 20-hydroxyecdysone (20E), using

a cell-based reporter gene assay (Figure 1). Ecdysone receptor agonists are used commercially as environmentally safe insecticides (Dhadialla et al., 1998; Sawada et al., 2003) and, more generally, compounds targeting nuclear receptors represent 13% of FDA-approved drugs (Overington et al., 2006).

RESULTS AND DISCUSSION

The Droplet-Based Microfluidic System

We used a droplet-based microfluidic system to measure the concentration-response profile for a nuclear receptor agonist, the hormone 20E, with a cell-based reporter gene assay (Figure 1). Binding of 20E to the ecdysone receptor (EcR, NRH1) (Koelle et al., 1991; Thomas et al., 1993; Yao et al., 1993) in *Bombyx mori* BM5 cells carrying a 20E-inducible green fluorescent protein (GFPS65T, hereafter referred to as GFP) results in the expression of GFP (Swevers et al., 2004). First, the hormone is mixed with a fluorescent dye (dextran Texas red; DTR) to encode the hormone concentration. Second, using a microfluidic device, the reporter cells are coencapsulated in droplets ($\sim 0.45 \pm 0.15$ cells per droplet) with eight or ten discrete hormone concentrations covering an ~ 3 decade concentration range generated by on-chip dilution of the hormone (Laval et al., 2007) (Figure 2; see Tables S1 and S2 available online). Other fluorescent droplet-encoding strategies can be found in the work of Brouzes et al. (2009) and Joensson et al. (2009). Droplets of ~ 900 pl volume are produced at ~ 0.3 kHz by flow focusing of the aqueous phase with a fluorinated oil phase (HFE7500; 3M) containing 0.5% (w/w) EA-surfactant (RainDance Technologies), a biocompatible PEG-PFPE amphiphilic block copolymer (Holtze et al., 2008). For each hormone concentration, droplets are generated for about 1 min ($\sim 7500 \pm 2500$ cells in $\sim 17,000$ droplets; Experimental Procedures). All the droplets (with the ten different levels of hormone concentration encoded by the dye) are collected in a single reservoir, a Pasteur pipette (Baret et al., 2009). Thus, in a single run, the effect of the ten concentrations of hormone on the cells is assayed simultaneously and under the same conditions. The generated emulsion is then incubated at room temperature for 24 hr (Figure 2E) and reinjected for fluorescence measurement at ~ 60 Hz (Figure 2F).

Microfluidic Measurement of the EC_{50} with the Dose-Response Curve

The fluorescence of the droplet and the cells are measured simultaneously on chips using a laser-induced fluorescence system (Figure 3A) and are represented as a two-dimensional histogram (Figures 3B and 3C). The fluorescence of the droplet (x axis; orange, DTR signal) encodes the hormone concentration, and the fluorescence of the cell (y axis; green, GFP signal) corresponds to its response. The orange fluorescence shows ten discrete levels corresponding to the ten concentrations of hormone, C, both at production and reinjection (Figures 3B and 3C). The populations have a 2% variation in orange fluorescence and are well separated, indicating good stability of the syringe pumps (see Figure S1 for details of the calibration of the coding system and a discussion of the difference in the fluorescence of the codes when measured on production and reinjection). At high hormone concentrations (above 27.6 nM, fifth to tenth populations), a cell population with high green-fluores-
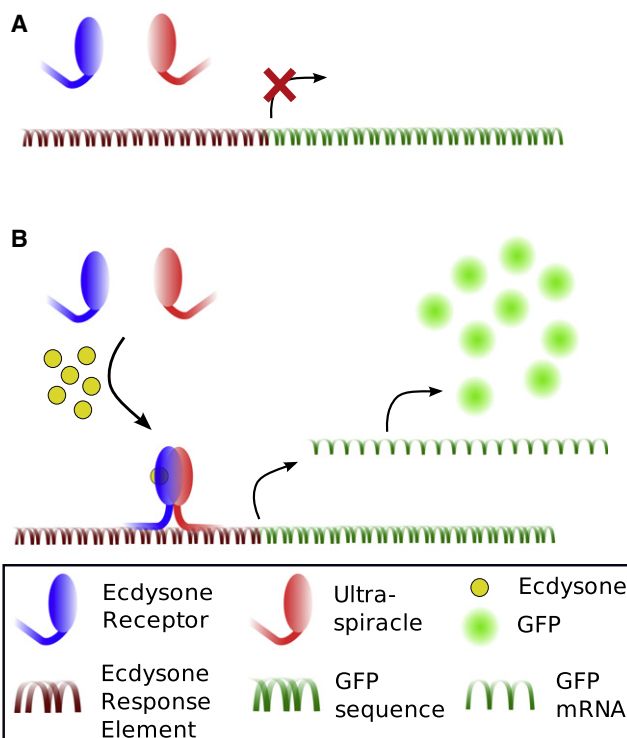

Figure 1. Cell-Based Reporter Gene Assay

The assay is based on the response of transformed *Bombyx mori* cells in the genome of which a transgene encoding green fluorescent protein under *ecdysone response element* control has been inserted. The cells endogenously express the ecdysone receptor (EcR, NRH1) and Ultraspiracle (USP, NR2B4), two nuclear receptors.

(A) In the absence of the hormone 20-hydroxyecdysone (20E), EcR and USP cannot form the active complex able to induce reporter gene expression (Swevers et al., 2004).

(B) In the presence of 20E, the EcR ligand, a complex constituted by EcR, 20E, and USP, specifically binds the *ecdysone response element* and induces GFPS65T gene expression.

cent intensity becomes visible. An epifluorescence micrograph of the droplets upon reinjection shows the different levels of orange fluorescence and green fluorescence of cells (Figure 3D). The response of the cells has a relatively wide distribution (over a decade), and there is always a population of nonresponding cells (see also Figure 3D). The heterogeneity of response is consistent with other studies of reporter gene expression at the single-cell level, in which large populations of cells displaying no response sustained rises in reporter activity, and transient phasic, or oscillatory, responses can be seen after stimuli (Takasuka et al., 1998; Norris et al., 2003). We attribute the relatively low ratio of responding cells in the microfluidic system ($\sim 10\%$ of total cells) to the use of adherent cells in suspension: the number of responding cells was $\sim 70\%$ when adherent cells were induced in microtiter plates and assayed by flow cytometry (in which case both adherent and nonadherent cells are assayed after resuspension), and $\sim 99\%$ when assayed directly in microtiter plates (in which case only adherent cells are measured) (Figure 4; Experimental Procedures). Indeed, it may be advantageous to cultivate adherent cells on microcarrier beads in
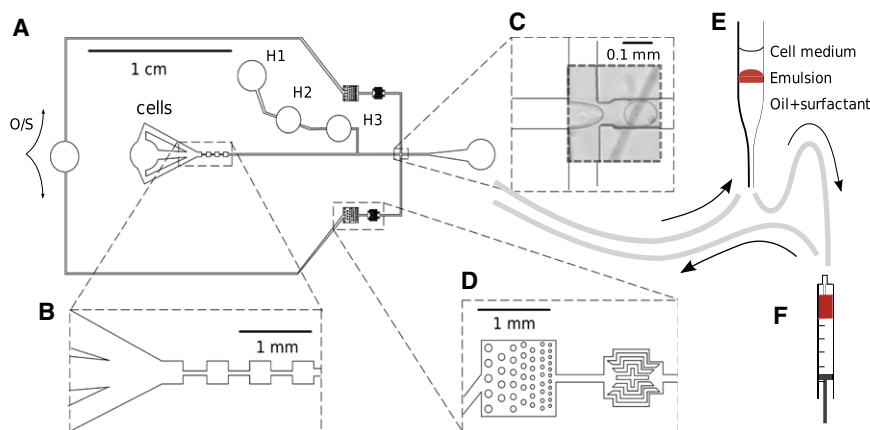
Figure 2. Device and Experimental Workflow

(A) General view of the microfluidic device for the coencapsulation of cells and hormone 20E. The emulsion is produced with the flow-focusing device using a mixture of oil and surfactant (O/S), and cells are cocompartmentalized with 20E. The hormone flows from three syringes containing different hormone concentrations; the final concentration in the droplet is determined by the relative flow rates (Q1, Q2, Q3) in the inlets H1, H2, and H3 (Tables S1 and S2). All the flow rates are controlled by syringe pumps.

(B) Zoom on the series of constrictions used to split cell clumps.

(C) Zoom on the flow-focusing junction with a micrograph of a cell being encapsulated.

(D) Zoom on the set of filters used to prevent dust from entering the device.

(E) The assay (Figure 1) is performed in droplets: the emulsion is collected in a Pasteur pipette for incubation at room temperature for 24 hr. The emulsion is sandwiched between a layer of medium and the oil/surfactant mixture used for emulsification.

(F) At the end of the incubation, the emulsion is reloaded in a syringe and flushed back into the original chip for laser-induced fluorescence measurement (the laser is shaped into a line; see Figure 3A for details of the optical setup).

droplets in microfluidic systems in order to avoid the need to assay adherent cells in suspension (Figure S2).

To circumvent this and account for responding cells only a threshold is defined (RFU green = $10^{1.5}$). Using a higher threshold (RFU green = 10^2) does not significantly change the calculated EC_{50} but decreases the number of cells analyzed. Formally, the response R of the cells is defined as the mean value of the fluorescent signals detected beyond this threshold. Despite the large standard deviation of cell fluorescence (on the order of the R), the large number of data points results in a ±8% confidence limit for the mean (α = 0.05) for all hormone concentrations tested (Figure 5A). The Z′ factor, Z′ = 0.86, of the assay in droplets, representing the efficiency of the screening of potential drugs using the reporter system, is calculated using the most extreme concentrations (C = 0.66 nM and C = 273 nM) as negative and positive controls (Experimental Procedures) and makes this an excellent assay for screening chemical compounds (Zhang et al., 1999). By fitting R versus the hormone concentration, C, with a four-parameter Hill function, EC_{50} values were determined and ranged from 53 to 85 nM in four independent experiments. The intraexperimental precision of the EC_{50} in each case is ±8% (α = 0.05) and the interexperimental precision for the mean EC_{50} (70 nM) is ±12% (α = 0.05). These EC_{50} values are in close agreement with EC_{50} values determined in microplates (40–49 nM), using flow cytometry (87 nM) (Experimental Procedures; Figure 5A), and with the literature (EC_{50} = 75–100 nM) (Swevers et al., 2004). The droplet-based experiments led to EC_{50} values intermediate between plates and flow cytometry, and the general shape of the dose-response curve (including the exponent) was similar for all methods and experiments (Figure 5A). This indicates that there is no significant diffusion of hormone either out of droplets or between droplets.

Reducing the Number of Cells Required Compared to Conventional Systems

Already, using eight hormone concentrations and 7500 cells per concentration, with ~0.5 cells per droplet and with a droplet

reinjection rate of 60 Hz, EC_{50} values are determined in ~30 min, using a total of only ~60,000 cells. This compares to 2.10^6 cells for an EC_{50} determined using flow cytometry or microtiter plates (assuming that 2.10^5 cells are induced per microtiter-plate well at each of ten hormone concentrations before measurement using flow cytometry or image analysis) (Experimental Procedures). Decimation of the data shows that ten times fewer cells are sufficient to measure EC_{50} (Figure 5B): using a total of only ~6000 cells, the throughput can easily be increased by a factor of 10 for a robust measurement of EC_{50} in ~3 min. A further increase in throughput could be achieved by optimization of droplet size for reinjection: rates of 500 Hz have been achieved for 660 pl droplets (Clausell-Tormos et al., 2008) and rates up to 2 kHz have been demonstrated for even smaller droplets (Baret et al., 2009), which would increase throughput up to ~30-fold and allow the determination of an EC_{50} in ~6 s. The throughput could also be increased by increasing the fraction of responding cells; for example, strategies could be implemented for the manipulation of adherent cells, such as on-chip cultivation before encapsulation (Hufnagel et al., 2009) or cultivation on microcarrier beads to provide a solid support to the cell in the droplets (see Figure S2). Finally, although in the range of flow rates used in our experiment syringe pump accuracy was not a limiting factor (see Figure S1), the use of three different pumps to produce the whole range of dilution series could be an obstacle to the generalization of our approach. On-chip dilution systems taking advantage of laminar flow profiles in networks of channels could be used to create droplets containing different concentrations of the test compound in a more convenient way (Damean et al., 2009), thereby facilitating the screening of compound libraries loaded from microtiter plates using a robotic autosampler (Clausell-Tormos et al., 2010).

Future Perspectives

Droplet-based microfluidic systems provide a quantitative and automated method to measure dose-response profiles using
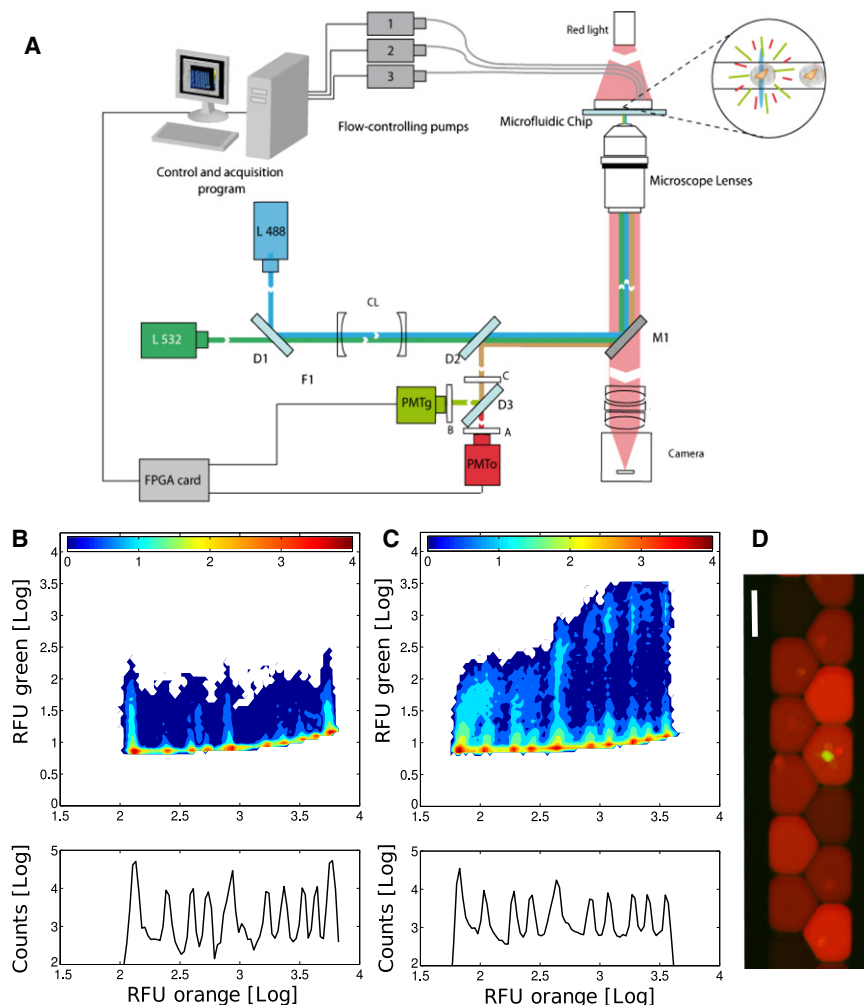
Figure 3. Fluorescence Measurement and Data Analysis

(A) A sketch of the fluorescence setup used for the detection of cell GFP fluorescence in droplets labeled by the fluorescent dye dextran Texas red (DTR). The setup is based on fluorophore excitation by two lasers (blue L488 and green L532) focused in the microfluidic channels. Emission is measured simultaneously on two photomultiplier tubes (PMT) in the green and orange windows of the light spectrum (see Experimental Procedures for details of the optical components).

(B) Two-dimensional histogram of droplet/cell fluorescence measured at droplet production. On the x axis, the histogram reveals the ten levels of concentration of DTR encoding the ten levels of 20E (Table S1 and Figure S1). The y axis represents GFP fluorescence.

(C) Two-dimensional histogram of droplet/cell fluorescence after incubation; a second green fluorescent population is visible for the highest concentration of DTR and 20E representing the concentration-dependent response of the cells. The counts (bottom panels) are the logarithm of the number of cells detected at different levels of orange fluorescence (*RFU*).

(D) Epifluorescence microscopy of droplets upon reinjection showing the green fluorescence (GFP) of the cell in the droplet and various orange intensities of the droplet corresponding to different concentrations of DTR and 20E. DTR concentrations span an ∼100-fold concentration range (Figure S1); the dark droplets correspond to low concentrations of DTR and the brighter droplets to higher concentrations of DTR. The scale bar represents 100 μm.

droplets as microreactors and to determine EC_{50} values using cell-based reporter gene assays in droplets. The dose-response profile and EC_{50} in microfluidics are consistent with microtiter plate and flow cytometry measurements as well as the value reported in the literature. EC_{50} values can be automatically measured with as few as 6000 cells to obtain a complete dose-response profile in ∼3 min using >300 times fewer cells than used for an EC_{50} determined using flow cytometry or microtiter plates (2.10^6 cells). Assays such as the one demonstrated here, based on quantifying cellular transcriptional responses, require incubation times of 24 hr, but the same system could easily be adapted, by the use of on-chip delay lines (Song and Ismagilov, 2003; Frenz et al., 2009), to measure rapid cellular responses at the other end of the temporal spectrum such as receptor-mediated calcium signals, as well as to in vitro assays. Indeed, the platform can be generalized to perform most homogeneous fluorescence-based assays commonly performed in microtiter plates. Finally, the flexibility of droplet manipulation also enables more complex operations to be performed. For example, cells can be preincubated in droplets with test compounds and then assay reagents can be added via drop fusion before readout (Brouzes et al., 2009), which would increase the range of assays that can be performed in droplet-based format.

SIGNIFICANCE

Nowadays, functional cell-based assays represent approximately half of all high-throughput screens (HTS) performed, and are an essential tool for chemical biology and chemical genetics approaches to identify new drug targets and small molecules of potential medical value. However, in a classical HTS, usually just a single measurement at a single concentration is obtained for each compound in the primary screen, whereas biological effects of chemical compounds can exhibit complex concentration-dependent relationships varying in potency, efficacy, and steepness of response. Using a droplet-based microfluidic system, we measured dose-response profiles precisely and quantitatively, at the single-cell level, using a reporter gene assay. Droplets—microcompartments of about 1 nl (1000-fold smaller than the smallest working volumes in microtiter-plate wells)—manipulated and analyzed at kHz rates function as microreactors for the analysis of single cells and chemical compounds. This system provides a new way to perform quantitative cell-based assays on small numbers of cells: dose-response profiles and EC_{50} values were automatically measured with as few as 60,000 cells and data from only
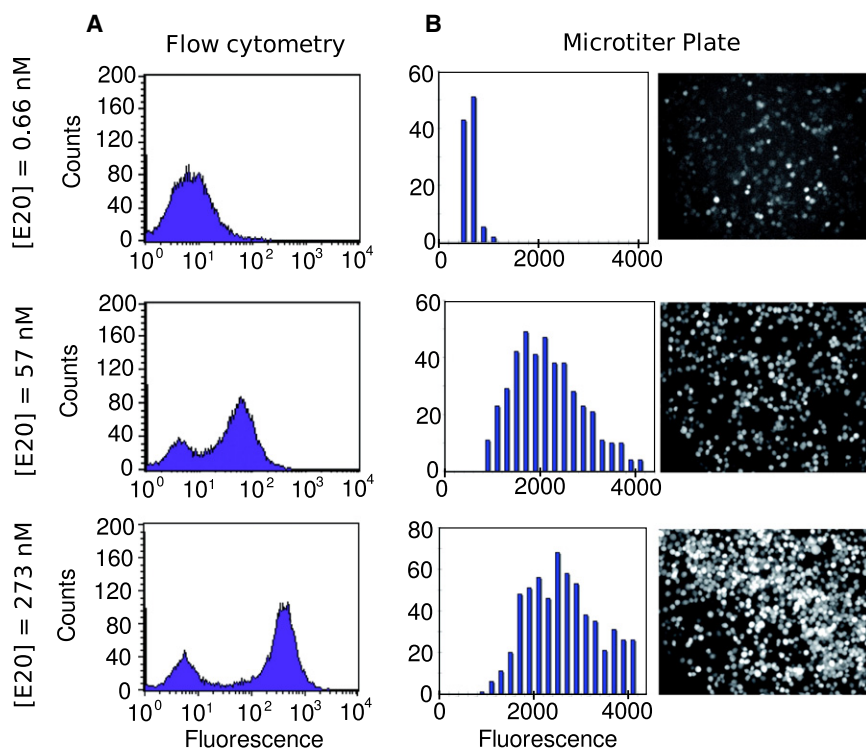
Figure 4. Cell-Based Reporter Gene Assay Using Standard Techniques

Fluorescence distribution of cells obtained by flow cytometry (A) and by measurement in microtitre plate (B) for cells incubated with 0.66, 57, and 273 nM 20-hydroxyecdysone. In both cases, the histograms are determined by the measurement of the fluorescence of single cells, either in flow (flow cytometry) or on the surface of the plate (using an IN Cell Analyzer).

ously (Clausell-Tormos et al., 2008) (Figures 2A–2D). Curing agent was added to the PDMS base (Sylgard 184 silicone elastomer kit; Dow Corning) to a final concentration of 10% (w/w), mixed, and poured over the mold to a depth of ~5 mm. Following degassing for several minutes and crosslinking at 65°C for several hours, the PDMS was peeled off the mold and the input and output ports were punched with a 0.75 mm diameter biopsy punch. In total six holes were punched: one inlet for the oil stream, one inlet for the medium stream carrying the cells, three inlets for the medium stream containing the hormone, and one outlet. Particles of PDMS were cleared from the ports using pressurized nitrogen gas and Scotch tape. The structured side of the PDMS slab was bonded to a 75 × 50 × 1.2 mm glass microscope slide (Millipore) by exposing both parts to an oxygen plasma (PlasmaPrep 2 plasma oven; GaLa Instrumente GmbH) and pressing them together. Finally, an additional hydrophobic surface coating was applied to the microfluidic channel walls by injecting the completed device with Aquapel glass treatment (PPG Industries) and then purging the liquid with nitrogen gas. The same device was used for cell encapsulation upon droplet production and droplet reinjection after incubation: droplets were reinjected through the outlet of the production device.

Microfluidic Droplet Manipulation

Liquid flow in the microfluidic channels was controlled by Harvard Apparatus syringe pumps (PHD 22/2000), and controlled via a Labview interface (home-made using the original pump drivers).

Cell Encapsulation

The emulsion was generated by co-flowing an oil stream (HFE7500; 3M]; Qo = 2.5 ml/hr) containing a droplet-stabilizing surfactant (EA, 0.5%, w/w; RainDance Technologies) with an aqueous stream which provides a biocompatible environment for the cells (Clausell-Tormos et al., 2008; Holtze et al., 2008). The aqueous stream (total flow rate 1 ml/hr) combined four streams, one cell stream at a constant flow rate of 0.5 ml/hr from a 5 ml B. Braun syringe and three streams connected to three different 1 ml Omnifix syringes containing different hormone and DTR concentrations (the syringes contained ~1 ml of liquid at the beginning of the experiments): 0 nM 20E with 1 µM DTR, 60 nM 20E with 10 µM DTR, and 600 nM 20E with 100 µM DTR (Figure 2A). The sum of the three flow rates was constant ($Q_1 + Q_2 + Q_3$ = 0.5 ml/hr) but the relative flow rates of each stream provide various hormone and dye concentrations (Tables S1 and S2). BM5 cells were harvested and then centrifuged 1 min at 90 × g. The pellet was resuspended in fresh medium to give ~10^6 cells per ml in the syringe. Emulsions were produced with eight or ten levels of dyes and hormone concentration. For each set of flow rates, the fluorescent signal of the dye measured was as expected from basic dilution calculation (data not shown). Each flow rate condition was maintained for a defined time (≥1 min) to collect sufficient droplets to enable statistical analysis (~17,000 droplets) (Table S3). We switched manually between two concentrations, which resulted in a stabilization time on the order of a few seconds, smaller than the smallest collection time (~1 min). Transient states are therefore
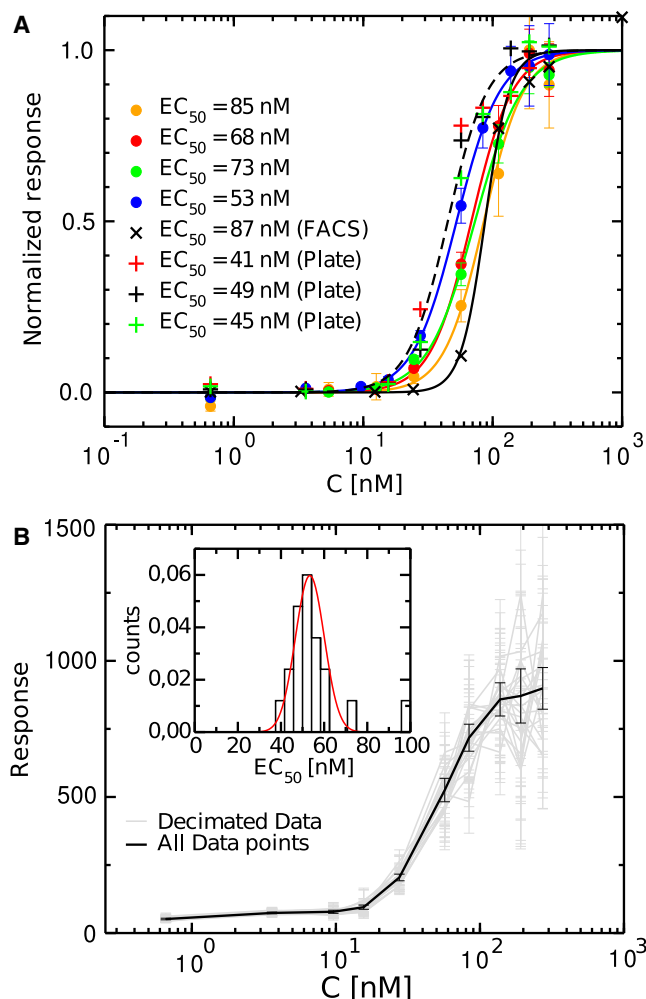
6000 cells were sufficient to determine the EC_{50}. This is >300 times fewer cells than required for an EC_{50} determined using flow cytometry or microtiter plates (2 × 10^6 cells). This hybrid system combines the advantages of flow cytometry (high-throughput single-cell analysis) and microtiter plates (compartmentalization of assays). We believe that miniaturization and automation of cell-based assays using droplet-based microfluidics open the door to the quantitative screening of compounds in droplet-based formats, and will enable chemical compound screening using cell types that are difficult or expensive to obtain in large quantities such as primary or stem cells and with small amounts of reagents for a drastic reduction in the cost of assays.

EXPERIMENTAL PROCEDURES

Cells and Culture Medium

B. mori BM5 cells carrying a 20E-inducible green fluorescent protein (GFP) reporter construct (*Bm5/ERE.gfp*) (Swevers et al., 2004) were cultured in enriched IPL-41 medium (Invitrogen) supplemented with 10% inactivated fetal bovine serum. Cell density was determined by hemocytometry. Before counting, cells were harvested and centrifuged for 1 min at 90 × g. After resuspension of the pellet in fresh medium, a fraction of the culture was diluted twice in a solution of trypan blue (0.4% w/v) in order to discriminate dead and living cells. The appropriate volume of culture medium was then added to the cell culture to obtain a final concentration of 10^6 cells/ml.

Device Processing

Each microfluidic device was prepared from poly(dimethylsiloxane) (PDMS) by standard soft-lithography techniques (Xia and Whitesides, 1998). A mold of SU-8 resist (MicroChem)—75 µm thick—was fabricated on a silicon wafer (Siltronix) by UV exposure (MJB3 contact mask aligner; SUSS MicroTec) through a photolithography mask and developed (SU-8 developer; Micro-Chem). The design has already been used successfully as described previ-

Figure 5. EC_{50} Measurement and Data Analysis of the Droplet-Based Experiment

The two-dimensional histogram enables a dose-response profile of the hormone to be measured.

(A) Dose-response curve extracted from experiments. The response of the cells is defined as the mean value of cell green fluorescence above $10^{1.5}$ RFU. The experiments have been reproduced on eight or ten levels of hormone concentrations leading to similar EC_{50} values (dots). The results are compared to those from flow cytometry (x) and microtiter plates (three independent experiments) (+) and are in good agreement. The fit of the plate experiment (dashed line) is only given for a single experiment (EC_{50} = 45 nM) for clarity (Tables S5 and S6). The error bars of the droplet-based experiments correspond to the 95% confidence interval of the mean.

(B) Decimation test: we produced 20 sets of data by randomly picking one data point out of ten. The EC_{50} values obtained by the fit of the data with a Hill function follow a Gaussian distribution centered on the EC_{50}. The dispersion of the results shows that a robust EC_{50} determination is achieved using ten times fewer cells than the number used in the present experiments, which indicates that a 10-fold increase in throughput is achievable.

neglected. The flow rates and device used resulted in droplet production by flow focusing (Anna et al., 2003) at a frequency of ~0.3 kHz which led to a droplet volume of about ~0.8–1 nl. The estimate of the average number of cells per droplet was therefore ~0.3–0.6. However, a certain level of cell clumping has been observed, which slightly decreased the cell occupancy in droplets. Syringes were connected to the microfluidic device using 0.6 × 25 mm Neolus needles (Terumo) and PTFE tubing with an internal diameter

of 0.56 mm and an external diameter of 1.07 mm (Fisher Bioblock Scientific). However, for these experiments, we preferred to remove all metal parts with small internal diameter to improve droplet stability and decrease the hydrodynamic stress on the cells. We also found that cells can accumulate in the needles, which limits the use of the needles. In order to connect the syringes to tubing, we shaped PDMS discs (5 mm thick) to the diameter of the syringe and biopsy punched a hole. The PDMS disk was then inserted into the syringe using the syringe piston. This enables a reversible connection between the PTFE tubing and the syringe. This system was tight, provided that the PDMS disk was slightly wider than the syringe. This method was used both for cell encapsulation and for droplet reinjection. A Teflon-coated magnet was added to the syringe containing the cells to ensure mixing: all the volume in the syringe (~3 ml at the beginning of the experiment) was permanently under agitation acting against cell sedimentation.

Incubation

The generated emulsion flowed off-chip through an ~40 cm length of PTFE tubing to a glass Pasteur pipette containing a few hundreds of microliters of cell medium (Figure 2E) (Baret et al., 2009). The emulsion was collected underneath the less dense medium for ~20 min, yielding a total volume of ~0.5 ml. The PTFE tubing was sealed and the pipette was incubated at room temperature for 24 hr. A single Pasteur pipette was used to collect all the droplets produced with the different hormone concentrations. The layer of medium above the emulsion was necessary to prevent evaporation and coalescence, but still allowed gas exchange with the atmosphere. Gas exchange was essential for the assay. In the collection pipette, layers of droplets of different colors were visible, indicating that there was neither flow nor mixing of the droplets during incubation.

Droplet Reinjection

Reinjection was a two-step process (Figure 2F). The Pasteur pipette was first connected through the PTFE tubing to a 1 ml Omnifix syringe and the emulsion was sucked in the syringe (at 2 ml/hr). The emulsion was then pushed back into the microfluidic device at a flow rate of 0.2 ml/hr. We used the same device design for reinjection for convenience and spaced the reinjected droplets with a stream of pure oil (HFE7500) at 1 ml/hr. The spacing was required to have a sufficient resolution of droplet detection. Droplet frequency upon reinjection was ~60 Hz (one fifth of droplet production rate). Detailed analysis of the fluorescence data revealed that the brightest population was less present at reinjection compared to production: it was the first to be reloaded into the device and was used for the alignment of the optics with the device and device calibration. However, because a large excess of this population was produced, sufficient data were collected for that particular point. Note that we collected an excess of the brightest and darkest populations as well as one intermediate population as quality control of the production/incubation/reinjection process: the proportion of droplets for each concentration step at reinjection was consistent with the proportions at production (Table S3). We did not observe any significant change in the fluorescent code during incubation, for example through the exchange of dye between droplets (Figure S1). We determined a coalescence rate of about 8% (Table S7 and Figure S3). We have previously shown that droplets of similar composition and volume (660 pl) can be reinjected after 15 days of incubation with no sign of increased coalescence during incubation compared to earlier time points (Clausell-Tormos et al., 2008) and that smaller droplets of ~100–200 pl can be reinjected after 1 year of storage at room temperature without seeing any major impact on droplet size distribution. Hence, we believe that the droplet coalescence we observe most likely occurs during manipulation of the droplets and not during incubation.

Optical Setup, Data Acquisition, and Control System

The optical setup (Figure 3A) consisted of a Leica inverted microscope mounted on a vibration-dampening platform (Thorlabs GmbH). A 20 mW, 488 nm solid-state laser (Spectra-Physics Cyan; L488) and a 532 nm laser (CrystaLaser CL2000; 50 mW, L532) were combined via a dichroic mirror (D1 = Di01-R488-25x36; Semrock) and a set of mirrors (M = BB1-E02; Thorlabs GmbH). The laser beams were shaped into an ~10 × ~150 μm line by a combination of a 25 mm diameter cylindrical lens (CL = LJ1878L2-A + LJ1653L1-A; Thorlabs GmbH). This laser line was required to enable the

excitation of all cells in droplets regardless of their position in the droplets. At the detection point the droplets were constrained, as the channels were slightly more narrow than the droplets. However, we did not use an additional constriction in the reinjection channel in order to avoid droplet coalescence linked to decompression of the emulsion (Bremond et al., 2008). Inside the microscope, the laser light was reflected up into an LD Plan Neofluar 40×/0.55 microscope objective and focused across a channel within the microfluidic device. A Guppy camera (Allied Vision) was mounted on the top camera port of the microscope to capture digital images during droplet manipulation. Light emitted from fluorescing droplets was captured by the objective and channeled back along the path of the laser. The emitted light was separated from the laser beam by a 488/532/638 nm wavelength-transmitting dichroic beam splitter (D2 = Di01-T488/532/638-25x36x5.0; Semrock) passed through a 488 nm and a 532 nm notch filter (C = NF01-488U-25 + NF01-532U; Semrock). Fluorescent light was decomposed into two components, green and orange by a dichroic mirror (D3 = FF562-Di02-25x36). Each component was then filtered through a set of filters and lenses (B = FF01-625/26 [Semrock] + AC254-030-A1 [Thorlabs GmbH] C = FF01-514/30 [Semrock] + AC254-030-A1 [Thorlabs GmbH]) and collected in two H5784-20 photomultiplier tubes (Hamamatsu Photonics; PMTg and PMTo). The gains on the photomultiplier tubes are optimized to detect fluorescence over a 3 log range. For fully induced cells, a very limited number of saturated events are observed and they do not modify the mean value of the cell fluorescence: less than 1% of droplets above the threshold are saturated events (66 out of 7811). Data acquisition (DAQ) and control were performed by a PCI-7831R Multifunction Intelligent DAQ card (National Instruments) executing a program written in LabView 8.2 (National Instruments). The data acquisition rate for the system was 100 kHz. Green and orange fluorescence of each droplet was measured as well as droplet width (corresponding to its diameter) and saved. Data processing, histograms, and color plots were then performed using a homemade Matlab code. The measurement of the droplet width enabled split droplets (smaller) or fused droplets (larger) to be removed from the analysis. The photomultiplier tube returns a voltage U depending on the gain G applied to the PMT. In order to compare values of U obtained for different gains, we defined the relative fluorescence unit (RFU) as $RFU = U/G^{7.2}$, with U and G expressed in volts. The exponent 7.2 was given by the PMT manufacturer and has been checked experimentally. In the range of concentrations used in the experiments, the green fluorescence of the droplet slightly increased with the orange signal as the result of optical leakage of DTR fluorescence into the green PMT; this effect was sufficiently small not to interfere with the assay.

Signal Analysis

Two populations were visible on the green fluorescence signal of the two-dimensional histograms, one corresponding to both empty droplets and negative cells (cells that have not been induced, such as, for example, dead cells) and the other one corresponding to positive cells (i.e., cells that have been induced) in droplets. A threshold was defined above which the cells are positive (here the value chosen was $RFU = 10^{1.5}$). Table S3 summarizes the statistics of the number of cells in droplets. As previously mentioned, the number of droplets measured at reinjection is the same as measured at encapsulation within 10%–20% except for the two extreme populations used for calibration of the optical setup. The response of the cells R was defined as the mean value of the "positive-cell" fluorescence and was extracted for each concentration. The actual standard deviation of the green fluorescence data of the cells was very large (on the order of the mean value of the fluorescence itself). Thanks to the large (>100) number of events detected, the 95% confidence interval of the mean based on a z test is much smaller (~±8%) at all hormone concentrations tested. The error bars of the dose-response plots (Figure 5A) correspond to this 95% confidence interval ($\alpha = 0.05$).

Z′ Factor

The positive control for the assay was the experiment performed with the highest hormone concentration ($C = 270$ nM); the negative control was the one with the lowest hormone concentration ($C = 0.66$ nM). For the four replicate experiments, we obtained different values of the normalized response R, summarized in Table S4. From these values, we determined the average value $\langle R \rangle$ of the normalized response and the standard deviation σ for the negative (n) and positive (p) control. These values enabled the $Z′$ factor, $Z′$, of the assay

to be determined based on the values of the controls (Zhang et al., 1999) according to Equation 1:

$$\langle EC_{50} \rangle = \frac{1}{n} \sum_{i=1}^{n} EC_{50}^{i}. \tag{1}$$

$Z′ = 0.86$ is a value corresponding to an excellent assay, usable in high-throughput screening.

Dose Response and EC_{50} Measurement

In order to determine the EC_{50}, we performed a fit of the dose-response data with a four-parameter Hill function (Equation 2):

$$R = a_0 + a_1 \frac{C^{a_2}}{C^{a_2} + EC_{50}^{a_2}}, \tag{2}$$

where R is the response of the cells measured experimentally and a_0, a_1, a_2, and EC_{50} are the fitting parameters. When several experiments are displayed on the same graph, the normalized response of the cells $R′ = (R - a_0)/a_1$ (Equation 3) enables data to be compared (Figure 5A):

$$R′ = \frac{C^{a_2}}{C^{a_2} + EC_{50}^{a_2}}. \tag{3}$$

The values obtained for the droplet-based experiments are summarized in Table S5. The intraexperimental 95% confidence interval on the fitted EC_{50} value, obtained using the commercial software PRISM, equals ±8% around the EC_{50}.

Confidence Interval for EC_{50}: Interexperiment

Based on the n = 4 experiments performed in the droplet-based format, we calculated the 95% confidence interval of the EC_{50} for different experiments. The values obtained for the EC_{50} are summarized in Table S5. The estimate of the mean is $\langle EC_{50} \rangle = 1/n \sum_{i=1}^{n} EC_{50}^{i}$ and the nonbiased estimate of the variance is $S^2 = 1/|n - 1| \sum_{i=1...n} (EC_{50}^{i} - \langle EC_{50} \rangle)^2$. Using the Student's t distribution with (n − 1 = 3) degrees of freedom, we obtained a ±12% width for the 95% confidence interval ($\alpha = 0.05$). This interexperimental confidence interval was then larger than the intraexperimental confidence interval (±8%; see above).

Decimation

In order to test the robustness of our approach and determine the minimum number of cells and time required for the assay, we made 20 random decimations of our data and plotted the 20 corresponding dose-response curves (Figure 5B). Because of the reduction in data points, the 95% confidence interval of the mean fluorescence value at each hormone concentration tested increases to ±24% but the distribution of the EC_{50} values is Gaussian (Figure 5B, inset) with mean equal to the EC_{50} ± 25% ($\alpha = 0.05$). The two sets of data returning the highest EC_{50} would have been discarded as outliers in a screening procedure because the fit with a Hill function was not reliable. These results show that throughput can easily be increased by a factor of 10 for a robust determination of EC_{50} in ~3 min using a total of only ~6000 cells.

Analysis by Flow Cytometry

In ten wells of six-well plates, 2.10^6 BM5 cells per well were incubated 24 hr in 2 ml of culture medium containing 0, 0.66, 3.3, 12.3, 24.3, 57, 111, 192, 273, or 1000 nM 20-hydroxyecdysone (SciTech). After incubation, cells were centrifuged 1 min at 90 × g and then each pellet was resuspended in 2 ml fresh medium. Each sample was filtered to remove millimeter-sized aggregates before analysis with a FACSCalibur flow cytometer using Cell Quest Pro 5.2.1 software (Becton Dickinson) (Figure 4A). The response of the cells is the mean value of the green fluorescence of the positive population (measured for each concentration over ~15,000 cells), as in the droplet-based experiment (Figure 5), and the dose-response data were then fitted by a four-parameter Hill function to extract the EC_{50}.

Analysis in Microtiter Plates

In 27 wells of a 96-well plate, 2.10^5 BM5 cells per well were incubated in 90 μl of culture medium. After overnight incubation at 28°C, 10 μl of culture medium

containing 20E to give a final concentration of 0.66, 3.6, 15.6, 27.6, 57, 84, 138, 192, or 273 nM was added to each well. For each hormone concentration, induction was performed in triplicate. The 96-well plate was placed in an IN Cell Analyzer 1000 (GE Healthcare) to take images of a 0.603 mm^2 area of each well, containing between 300 and 800 cells, every 20 min for 24 hr (Figure 4B). For this study, only the images corresponding to the 24 hr time point of each well were analyzed, using the software ImageJ (National Institutes of Health). The fluorescence intensity was individually measured for every cell in each image. The mean fluorescence intensity of the cells was used as the response to plot concentration response curves. These curves were fitted with a four-parameter Hill function (see Table S6) to obtain EC_{50} values (Figure 5A).

SUPPLEMENTAL INFORMATION

Supplemental Information includes three figures and seven tables and can be found with this article online at doi:10.1016/j.chembiol.2010.04.010.

REFERENCES

Agresti, J.J., Antipov, E., Abate, A.R., Ahn, K., Rowat, A.C., Baret, J.-C., Marquez, M., Klibanov, A.M., Griffiths, A.D., and Weitz, D.A. (2010). Ultra-high-throughput screening in drop-based microfluidics for directed evolution. Proc. Natl. Acad. Sci. USA 107, 4004–4009.

Ahn, K., Agresti, J., Chong, H., Marquez, M., and Weitz, D.A. (2006a). Electro-coalescence of drops synchronized by size-dependent flow in microfluidic channels. Appl. Phys. Lett. 88, 264105.

Ahn, K., Kerbage, C., Hunt, T.P., Westervelt, R.M., Link, D.R., and Weitz, D.A. (2006b). Dielectrophoretic manipulation of drops for high-speed microfluidic sorting devices. Appl. Phys. Lett. 88, 024104.

An, W.F., and Tolliday, N.J. (2009). Introduction: cell-based assays for high-throughput screening. Methods Mol. Biol. 486, 1–12.

Anna, S., Bontoux, N., and Stone, H. (2003). Formation of dispersions using "flow focusing" in microchannels. Appl. Phys. Lett. 82, 364–366.

Baret, J.-C., Miller, O.J., Taly, V., Ryckelynck, M., El-Harrak, A., Frenz, L., Rick, C., Samuels, M.L., Hutchison, J.B., Agresti, J.J., et al. (2009). Fluorescence-activated droplet sorting (FADS): efficient microfluidic cell sorting based on enzymatic activity. Lab Chip 9, 1850–1858.

Bremond, N., Thiam, A.R., and Bibette, J. (2008). Decompressing emulsion favors coalescence. Phys. Rev. Lett. 100, 024501.

Brouzes, E., Medkova, M., Savenelli, N., Marran, D., Twardowski, M., Hutchison, J.B., Rothberg, J.M., Link, D.R., Perrimon, N., and Samuels, M.L.

(2009). Droplet microfluidic technology for single-cell high-throughput screening. Proc. Natl. Acad. Sci. USA 106, 14195–14200.

Chabert, M., and Viovy, J.L. (2008). Microfluidic high-throughput encapsulation and hydrodynamic self-sorting of single cells. Proc. Natl. Acad. Sci. USA 105, 3191–3196.

Chabert, M., Dorfmann, K.D., and Viovy, J.-L. (2005). Droplet fusion by alternating current (AC) field electrocoalescence in microchannels. Electrophoresis 26, 3706–3715.

Clausell-Tormos, J., Lieber, D., Baret, J.-C., El-Harrak, A., Miller, O., Frenz, L., Blouwolff, J., Humphry, K.J., Koster, S., Duan, H., et al. (2008). Droplet-based microfluidic platforms for the encapsulation and screening of mammalian cells and multicellular organisms. Chem. Biol. 15, 427–437.

Clausell-Tormos, J., Griffiths, A.D., and Merten, C.A. (2010). An automated two-phase microfluidic system for kinetic analyses and the screening of compound libraries. Lab on a Chip 10, 1302–1307.

Damean, N., Olguin, L.F., Hollfelder, F., Abell, C., and Huck, W.T.S. (2009). Simultaneous measurement of reactions in microdroplets filled by concentration gradients. Lab Chip 9, 1707–1713.

Dhadialla, T.S., Carlson, G.R., and Le, D.P. (1998). New insecticides with ecdysteroidal and juvenile hormone activity. Annu. Rev. Entomol. 43, 545–569.

Dove, A. (1999). Drug screening—beyond the bottleneck. Nat. Biotechnol. 17, 859–863.

Frenz, L., Blank, K., Brouzes, E., and Griffiths, A.D. (2009). Reliable microfluidic on-chip incubation of droplets in delay-lines. Lab Chip 9, 1344–1348.

Granieri, L., Baret, J.-C., Griffiths, A.D., and Merten, C.A. (2010). High-throughput screening of enzymes by retroviral display using droplet-based microfluidics. Chem. Biol. 17, 229–234.

Griffiths, A.D., and Tawfik, D.S. (2006). Miniaturising the laboratory in emulsion droplets. Trends Biotechnol. 24, 395–402.

Hill, A.V. (1910). The possible effects of the aggregation of the molecules of haemoglobin on its dissociation curves. J. Physiol. 40, 4–7.

Holtze, C., Rowat, A.C., Agresti, J.J., Hutchison, J.B., Angilè, F.E., Schmitz, C.H.J., Köster, S., Duan, H., Humphry, K.J., Scanga, R.A., et al. (2008). Biocompatible surfactants for water-in-fluorocarbon emulsions. Lab Chip 8, 1632–1639.

Hong, J., Edel, J.B., and de Mello, A.J. (2009). Micro- and nanofluidic systems for high-throughput biological screening. Drug Discov. Today 14, 134–146.

Huebner, A., Sharma, S., Srisa-Art, M., Hollfelder, F., Edel, J.B., and Demello, A.J. (2008). Microdroplets: a sea of applications? Lab Chip 8, 1244–1254.

Hufnagel, H., Huebner, A., Guelch, C., Guese, K., Abell, C., and Hollfelder, F. (2009). An integrated cell culture lab on a chip: modular microdevices for cultivation of mammalian cells and delivery into microfluidic microdroplets. Lab Chip 9, 1576–1582.

Inglese, J., Auld, D.S., Jadhav, A., Johnson, R.L., Simeonov, A., Yasgar, A., Zheng, W., and Austin, C.P. (2006). Quantitative high-throughput screening: a titration-based approach that efficiently identifies biological activities in large chemical libraries. Proc. Natl. Acad. Sci. USA 103, 11473–11478.

Joensson, H.N., Samuels, M.L., Brouzes, E.R., Medkova, M., Uhlén, M., Link, D.R., and Andersson-Svahn, H. (2009). Detection and analysis of low-abundance cell-surface biomarkers using enzymatic amplification in microfluidic droplets. Angew. Chem. Int. Ed. Engl. 48, 2518–2521.

Kelly, B.T., Baret, J.-C., Taly, V., and Griffiths, A.D. (2007). Miniaturizing chemistry and biology in microdroplets. Chem. Commun. (Camb.) 18, 1773–1788.

Koelle, M.R., Talbot, W.S., Segraves, W.A., Bender, M.T., Cherbas, P., and Hogness, D.S. (1991). The Drosophila EcR gene encodes an ecdysone receptor, a new member of the steroid receptor superfamily. Cell 67, 59–77.

Köster, S., Angile, F., Duan, H., Agresti, J.J., Wintner, A., Schmitz, C., Rowat, A.C., Merten, C.A., Pisignano, D., Griffiths, A.D., and Weitz, D.A. (2008). Drop-based microfluidic devices for encapsulation of single cells. Lab Chip 8, 1110–1115.

Laval, P., Lisai, N., Salmon, J.-B., and Joanicot, M. (2007). A microfluidic device based on droplet storage for screening solubility diagrams. Lab Chip 7, 829–834.

Link, D.R., Anna, S.L., Weitz, D.A., and Stone, H.A. (2004). Geometrically mediated breakup of drops in microfluidic devices. Phys. Rev. Lett. *92*, 054503.

Malo, N., Hanley, J.A., Cerquozzi, S., Pelletier, J., and Nadon, R. (2006). Statistical practice in high-throughput screening data analysis. Nat. Biotechnol. *24*, 167–175.

Mazutis, L., Araghi, A.F., Miller, O.J., Baret, J.-C., Frenz, L., Janoshazi, A., Taly, V., Miller, B.J., Hutchison, J.B., Link, D., et al. (2009). Droplet-based microfluidic systems for high-throughput single DNA molecule isothermal amplification and analysis. Anal. Chem. *81*, 4813–4821.

Ménétrier-Deremble, L., and Tabeling, P. (2006). Droplet breakup in microfluidic junctions of arbitrary angles. Phys. Rev. E Stat. Nonlin. Soft Matter Phys. *74*, 035303.

Norris, A.J., Stirland, J.A., McFerran, D.W., Seymour, Z.C., Spiller, D.G., Loudon, A.S.I., White, M.R.H., and Davis, J.R.E. (2003). Dynamic patterns of growth hormone gene transcription in individual living pituitary cells. Mol. Endocrinol. *17*, 193–202.

Overington, J.P., Al-Lazikani, B., and Hopkins, A.L. (2006). How many drug targets are there? Nat. Rev. Drug Discov. *5*, 993–996.

Pauwels, R. (2006). Aspects of successful drug discovery and development. Antiviral Res. *71*, 77–89.

Priest, C., Herminghaus, S., and Seemann, R. (2006). Controlled electrocoalescence in microfluidics: targeting a single lamella. Appl. Phys. Lett. *89*, 134101.

Sawada, Y., Yanai, T., Nakagawa, H., Tsukamoto, Y., Tamagawa, Y., Yokoi, S., Yanagi, M., Toya, T., Sugizaki, H., Kato, Y., et al. (2003). Synthesis and insecticidal activity of benzoheterocyclic analogues of *N′*-benzoyl-*N*-(*tert*-butyl)benzohydrazide: Part 3. Modification of *N-tert*-butylhydrazine moiety. Pest Manag. Sci. *59*, 49–57.

Song, H., and Ismagilov, R.F. (2003). Millisecond kinetics on a microfluidic chip using nanoliters of reagents. J. Am. Chem. Soc. *125*, 14613–14619.

Song, H., Tice, J.D., and Ismagilov, R.F. (2003). A microfluidic system for controlling reaction network in time. Angew. Chem. Int. Ed. Engl. *42*, 768–772.

Squires, T.M., and Quake, S.R. (2005). Microfluidics: fluid physics at the nanoliter scale. Rev. Mod. Phys. *77*, 977–1026.

Swevers, L., Kravariti, L., Ciolfi, S., Xenou-Kokoletsi, M., Ragoussis, N., Smagghe, G., Nakagawa, Y., Mazomenos, B., and Iatrou, K. (2004). A cell-based high-throughput screening system for detecting ecdysteroid agonists and antagonists in plant extracts and libraries of synthetic compounds. FASEB J. *18*, 134–136.

Takasuka, N., White, M.R., Wood, C.D., Robertson, W.R., and Davis, J.R. (1998). Dynamic changes in prolactin promoter activation in individual living lactotrophic cells. Endocrinology *139*, 1361–1368.

Tawfik, D.S., and Griffiths, A.D. (1998). Man-made cell-like compartments for molecular evolution. Nat. Biotechnol. *16*, 652–656.

Taylor, G.I. (1953). Dispersion of soluble matter in solvent flowing slowly through a tube. Proc. R. Soc. Lond. A *219*, 186–203.

Thomas, H.E., Stunnenberg, H.G., and Stewart, A.F. (1993). Heterodimerization of the *Drosophila* ecdysone receptor with retinoid X receptor and ultraspiracle. Nature *362*, 471–475.

Wu, M.H., Huang, S.-B., and Lee, G.-B. (2010). Microfluidic cell culture systems for drug research. Lab Chip *10*, 939–956.

Xia, Y.N., and Whitesides, G.M. (1998). Soft lithography. Annu. Rev. Mater. Sci. *28*, 153–184.

Yao, T.P., Forman, B.M., Jiang, Z., Cherbas, L., Chen, J.D., McKeown, M., Cherbas, P., and Evans, R.M. (1993). Functional ecdysone receptor is the product of EcR and Ultraspiracle genes. Nature *366*, 476–479.

Zhang, J.H., Chung, T.D., and Oldenburg, K.R. (1999). A simple statistical parameter for use in evaluation and validation of high-throughput screening assays. J. Biomol. Screen. *4*, 67–73.